ACS APPLIED MATERIALS & INTERFACES

www.acsami.org

Research Article

MoVN-Cu Coatings for In Situ Tribocatalytic Formation of Carbon-Rich Tribofilms in Low-Viscosity Fuels

Kelly Jacques, Asghar Shirani, Jesse Smith, Thomas W. Scharf, Scott D. Walck, Stephen Berkebile, Osman Levent Eryilmaz, Andrey A. Voevodin,* Samir Aouadi,* and Diana Berman*

Cite This: *ACS Appl. Mater. Interfaces* 2023, 15, 30070−30082

Read Online

ACCESS | Metrics & More | Article Recommendations

ABSTRACT: Inhibiting the tribological failure of mechanical assemblies which rely on fuels for lubrication is an obstacle to maintaining the lifetime of these systems with low-viscosity and low-lubricity fuels. In the present study, a MoVN-Cu nanocomposite coating was tribologically evaluated for durability in high- and low-viscosity fuels as a function of temperature, load, and sliding velocity conditions. The results indicate that the MoVN-Cu coating is effective in decreasing wear and friction relative to an uncoated steel surface. Raman spectroscopy, transmission electron microscopy, and electron-dispersive spectroscopy analysis of the MoVN-Cu worn surfaces confirmed the presence of an amorphous carbon-rich tribofilm which provides easy shearing and low friction during sliding. Further, the characterization of the formed tribofilm revealed the presence of nanoscale copper clusters overlapping with the carbon peak intensities supporting the tribocatalytic origin of the surface protection. The tribological assessment of the MoVN-Cu coating reveals that the coefficient of friction decreased with increasing material wear and initial contact pressure. These findings suggest that MoVN-Cu is a promising protective coating for fuel-lubricated assemblies due to its adaptive ability to replenish lubricious tribofilms from hydrocarbon environments.

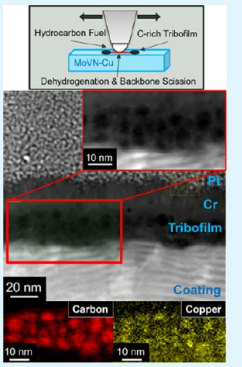

KEYWORDS: *tribocatalysis, ultralow wear, carbon, coatings, nitrides*

1. INTRODUCTION

A persistent issue within modern heavy-duty fuel engines is the tribologically induced wear and failure of components within the fuel injection system.[1] A wide range of strategies for decreasing the wear of contacting surfaces can be employed,[2] such as the inclusion of lubricity-aiding packages[3] and protecting surfaces with wear-resistant coatings.[4,5]

However, the methods available for reducing friction are limited in certain applications, such as the case for fuel injection systems that operate on low-lubricity fuels. For example, environmental restrictions concerning sulfur content within diesel fuels, such as those passed by the European Union in 2009, which limited the acceptable fuel sulfur content to 10 ppm.[6] One tribologically unfavorable consequence of the hydrotreating process leading to the extractions of sulfuric compounds from fuels is the simultaneous removal of various aromatic species from the fuel.[7] These aromatics are surfactants which form adsorbed films on metallic sliding interfaces, providing low friction and wear. Therefore, environmental restrictions over time have decreased the lubricating efficacy of diesel fuels. This reduction in lubricating ability provides a motive to determine novel and adaptive material solutions that improve the frictional behavior of fuel-lubricated mechanical assemblies via mechanisms unrelated to the deliberate inclusion of liquid surfactant species.[1,6] Within fuel injection systems, the fuel serves as a lubricant and friction reducer for moving components. However, conditions of elevated contact pressure that occur during engine operation may establish nonideal lubrication conditions, such as the boundary lubrication regime. When the lubrication between two solid bodies consists of low-viscosity, low-lubricity hydrocarbons such as ethanol, gasoline, and some synthetic fuels, the severity of the contact conditions and tribological damage experienced by these solid bodies can be exacerbated.[8] Consequently, the materials used to fabricate these fuel injection system components should resist wear in low-viscosity hydrocarbon fuels and therefore inhibit gross tribological failure in these challenging contact conditions.

Carbon-based films, such as graphene,[4,9] nanocrystalline diamond,[10−12] and diamond-like carbon (DLC),[13−18] have been widely employed to provide tribological protection to mechanical systems in various sliding configurations and environments. While the application of wear-resistant coatings increases the efficiency of mechanical components, these materials can fail due to delamination and wear when operated with fuels tailored for steel surfaces or low-viscosity fuels such as ethanol.[19−21] Truetler et al. evaluated several DLC coatings

Received: February 10, 2023
Accepted: April 25, 2023
Published: June 14, 2023

https://doi.org/10.1021/acsami.3c01953
ACS Appl. Mater. Interfaces 2023, 15, 30070−30082

employed in modern automotive fuel injection system components such as the piston, cylinder, and camshaft.[21] The study found evidence of tribologically induced DLC coating failure, noting that future fuel injection system designs would impose even greater pressure, load, temperature, and tolerance requirements for materials being exposed to low-lubricity fuels and more corrosive environments.[21] In similar studies, Hershberger et al., Radi et al., Bhowmick et al., and Ajayi et al. demonstrated the poor performance of DLC coatings when tribologically tested in low-lubricity liquids such as ethanol and synthetic diesel fuels.[19,20,22,23] Some degree of improvement in the DLC coating performance in fuels was achieved via increasing the surface roughness of the substrate materials, providing better adhesion and protection of the substrates from wear.[24,25] However, the roughening approach has limitations for systems, which require smooth component surfaces and tight tolerances between the components, such as in fuel injection systems.[21] The limitations of DLC coatings under conditions of low-viscosity lubrication shows the importance of developing new material solutions for resisting wear and friction in fuel-lubricated assemblies.

Often, the surfaces within fuel-lubricated systems are protected from tribological damage by facilitating interactions between complex fatty acids and heavy aromatic compounds within the fuel and the solid materials in the system.[7] In this case, the fatty acids and aromatic compounds protect surfaces by tribochemically adsorbing onto solid material surfaces. One of the most well-known tribochemical compounds is the zinc dialkyl dithiophosphate (ZDDP), included as an additive in oils.[26] ZDDP introduced in the sliding contact decomposes and forms a protective tribofilm on oil-lubricated alloy surfaces.[26] The implementation of ZDDP in oil-lubricated assemblies has been restricted due to emission legislation,[27] pushing researchers to explore alternative technologies.[28] Among solutions of interest are different ionic liquids and ashless organophosphate compounds.[29−31]

Recently, attention has shifted toward an alternative approach of the in situ generation of the surface protection, using tribocatalytic activity at the sliding contact.[32] Within sliding systems, intentional inclusion of catalytic species can be utilized to decrease the activation energy to initiate lubricity-aiding reaction processes on contacting surfaces. One such alternative is the addition of magnesium silicate hydroxide (MSH) nanoparticles into oils. Recent studies from Wang et al. and Chang et al. demonstrate the ability of MSH additives in oil to form protective tribofilms on steel surfaces.[33,34] While these lubricant additives are effective in protecting steel surfaces, there are applications for which modifications of the lubricant chemistry are not acceptable. In such cases, the tribocatalytic materials can be incorporated as components of protective coatings. These coatings with catalytically active inclusions can replenish the worn-away solid material with carbon-rich transfer films formed with the aid of a hydrocarbon environment, in forms of gas, liquid, or solid.[26,35,36] As a result, the lifetime of such tribocatalytic protective coatings is significantly extended and maintenance cost is reduced.

The concept of the tribocatalysis implies the in situ formation and repair of protective carbon films that is facilitated by the presence of catalytically reactive metals, such as Pt,[37−39] Ni,[40] Fe,[41] Mg,[42] etc., in the protective coatings. Specific examples of such coatings are MoN-Cu and VN-Cu produced by physical vapor deposition (PVD) methods that were recently shown to provide catalytic formation of carbon-rich films in polyalphaolefin (PAO), 5W30 formulated oil (contains zinc dialkyl dithiophosphate and other additives), and also in an alkyne environment.[28,43] Metal nitride-based hard coatings are known for their high toughness, wear resistance, and stability in corrosive and reactive environments,[44−46] and thus, their use as matrices for tribocatalytic element inclusion can provide the beneficial approach for surface engineering of fuel components to operate with low-viscosity hydrocarbons. There are also some efforts to explore other tribocatalytic systems, such as Pt−Au-based films,[37,38] that demonstrated tribocatalytic performance in low-viscosity alcohols and alcohol vapors. However, nitride-based coatings still offer the most reliable and economically viable protective approach. While the studies of Erdemir et al. and Shirani et al. demonstrate the protection of steel surfaces with tribocatalytic MeN-Cu coatings, these materials have yet to be tested for efficacy in low-viscosity fuels made of short-chain hydrocarbons, where ethanol, dodecane, decane, etc. are typical examples.[28,43] Additionally, previous research lacks practical evidence that the tribofilm formation occurs specifically on the Cu surfaces.[28]

In this study, MoVN-Cu metal nitride nanocomposite tribocatalytic coatings were evaluated for durability in high- and low-viscosity fuels as a function of temperature, load, and sliding velocity conditions. These MoVN-Cu coatings were subjected to ball-on-flat tribological experiments with initial contact pressures exceeding 1 GPa, at temperatures of 25 and 50 °C, reciprocating frequencies of 25 and 50 Hz, and in ethanol and dodecane fuel environments. The MoVN-Cu coating exhibited decreased wear and friction relative to uncoated AISI 52100 steel under these varying contact conditions. Tribofilm formation was observed in the presence of both ethanol and dodecane and was more pronounced in the dodecane environment. Transmission electron microscopy (TEM) analysis of the tribofilm indicated that the carbon-rich tribofilm is generated specifically on the Cu surfaces. The MoVN-Cu coating was notably adaptive in its tribological response under different normal loads (initial contact pressures of 0.82−1.25 GPa). The coefficient of friction during experiments was minimal when the initial contact pressure was at its maximum values, which is attributed to the increased generation of the low-friction tribofilm.

The results demonstrate great stability of the tribological performance of the MoVN-Cu tribocatalytic coating and show its versatility and durability for a wide range of tribological conditions. The well-established wear resistance and load support characteristics intrinsic to hard nitride coatings in combination with the novel adaptive catalytic tribofilm lubrication mechanism characteristic of the MoVN-Cu coating explored here provides a new approach for improving the wear endurance and performance of mechanical components handling low-viscosity fuels. This approach has the potential for considerably improving the lifetime of components within the fuel injection systems of emerging combustion engines, tailored for more environmentally benign low-viscosity hydrocarbon fuels.

2. EXPERIMENTAL PROCEDURE

2.1. Materials and Fuels. The materials used in this study include AISI 52100 steel, MoVN-Cu tribocatalytic coatings applied to an AISI 52100 steel substrate, and alumina (Al_2O_3) counterbodies. The lubricants/fuels used were ethanol and dodecane. AISI 52100 steel was selected as a tribological flat specimen and as the substrate

https://doi.org/10.1021/acsami.3c01953
ACS Appl. Mater. Interfaces 2023, 15, 30070−30082

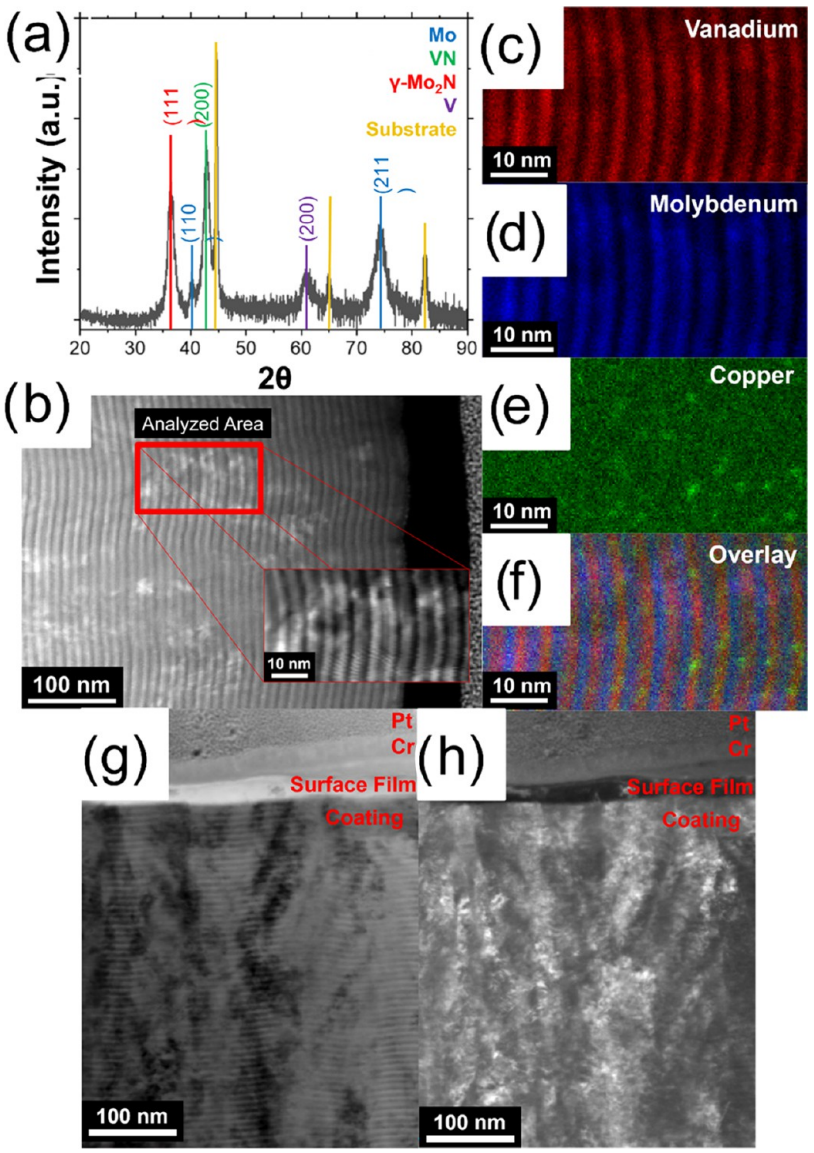

Figure 1. (a) Grazing-angle (α = 0.5°) XRD spectra of MoVN-Cu coating, (b) STEM-HAADF image of coating, and normalized XEDS spectral imaging (XEDS-SI) maps for (c) vanadium, (d) molybdenum, and (e) copper and (f) overlay image of all XEDS maps; (g) STEM bright-field (STEM-BF) and (h) STEM annular dark-field (STEM-ADF) images.

for the MoVN-Cu coating because it is representative of the alloys used in heavy-duty engine fuel systems.[47] Al_2O_3 was selected as the counterbody material due to its relative hardness and inert nature, allowing an assessment of the MoVN-Cu coating without additional chemical activity involved in metallic surfaces. The AISI 52100 steel flat specimen was through-hardened to a hardness value of 7.7 GPa and polished to an average surface roughness of 0.081 ± 0.02 μm. The hardness of the AISI 52100 steel was measured with a 500 g normal load and 20 indentations using a Wilson VH1102 (Buehler) Vickers hardness tester. The MoVN-Cu tribocatalytic coating was chosen for this study due to its high hardness and unique response to tribological contacts in the presence of hydrocarbons.[28] The hardness and elastic modulus of the MoVN-Cu coating was measured as 30.4 ± 4.1 and 347.2 ± 31.6 GPa with a MTS Nanoindenter XP equipped with continuous stiffness measurement (CSM) with 160 Nm indent displacements and a total of 40,000 indentations. The MoVN-Cu coating was deposited at 270 °C in a high-vacuum system by the direct current magnetron sputtering. The AISI 52100 substrates were etched with Ar ions prior to the deposition. The targets were pure Mo (99.95%), V (99.95%), and Cu (99.999%) deposited at the sputtering applied power of 9 W/cm^2 for Mo and V and 0.45 W/cm^2 for Cu. The Ar/N_2 ratio was 130−55 sccm at 0.4 Pa total pressure. The targets were rotated during the deposition to ensure the uniformity of the coating components. The resulting MoVN-Cu coatings have a thickness of approximately 600 nm and average surface roughness of 0.026 ± 0.006 μm. The surface roughness of the MoVN-Cu coating and the AISI 52100 steel was measured with a Dektak stylus profilometer. The counterbodies used for tribological experiments were polycrystalline Al_2O_3 balls with diameters of 6.00−6.35 mm. Ethanol and dodecane, the fuels used as lubricants during tribological experiments, have a viscosity at 40 °C of 1.08 and 7 cSt,[48,49] respectively. Dodecane was chosen as a fuel lubricant as it is a major component of kerosene-based fuels, such as those used in the aerospace industry,[50] and a minor component of diesel fuels. Ethanol was selected as an additional fuel for comparison because of its low viscosity relative to dodecane, polar nature, and poorer lubrication performance. Ethanol is also commonly added to gasoline fuels.

2.2. Measurement Method Overview. Reciprocating tribological experiments were conducted using a high-frequency reciprocating rig (HFRR) manufactured by PCS instruments. The experiments were conducted with various parameters to study the effect of sliding velocity, initial contact pressure, temperature, and

https://doi.org/10.1021/acsami.3c01953
ACS Appl. Mater. Interfaces 2023, 15, 30070−30082

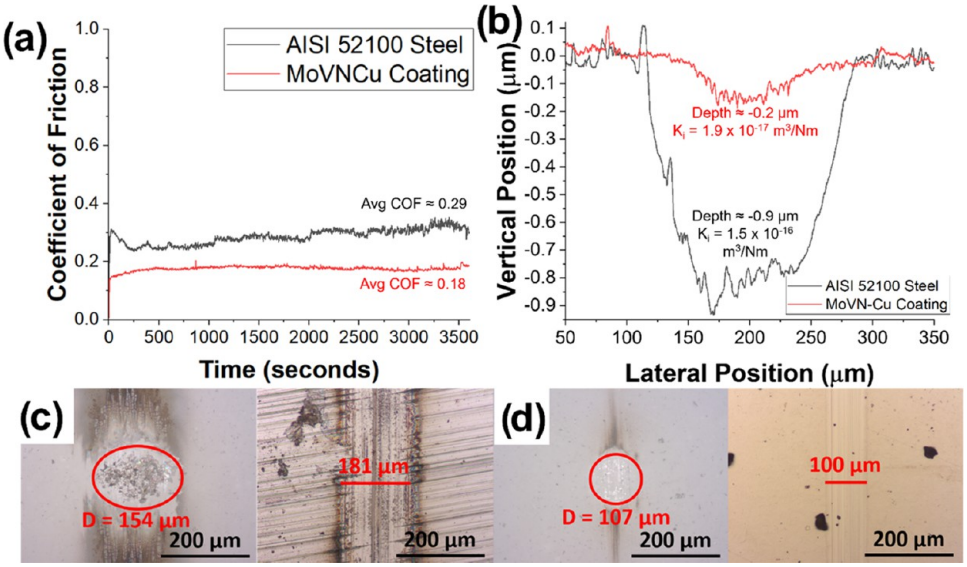

Figure 2. Comparison of (a) the coefficient of friction vs. time plots, (b) flat wear scar profiles, and (c, d) optical images of the AISI 52100 steel, MoVN-Cu coating, and Al_2O_3 counterbody wear scars. The experiments were conducted using AISI 52100 steel and MoVN-Cu-coated AISI 52100 steel flat surfaces, Al_2O_3 counterbodies, a normal load of 200 g, a frequency of 50 Hz, the stroke length of 1 mm, the temperature of 40 °C, ethanol as the lubricant, and a duration of 60 min.

type of lubrication on the tribological behavior of the MoVN-Cu coating. Each tribological experiment was performed at least two times to ensure the reproducibility of the results. The initial contact pressures used were 0.82, 1.11, and 1.25 GPa, which correspond to the applied normal loads of 200, 500, and 700 g. The stroke length for the experiments was 0.5 mm, and reciprocating frequencies of 25 and 50 Hz were used. The average sliding velocities were 0.025 and 0.050 m/s, the temperatures used were 25 and 50 °C, the relative humidity was approximately 40% in the specimen environment, and the lubricants used were ethanol and dodecane.

After tribological experiments were performed, the material surfaces were characterized by various methods. Nanoindentation mapping of the worn surfaces was performed with a sample size of 40,000 indents, 15−25 mN load, and 1.5−3.5 μm spacing for the MoVN-Cu coating and uncoated 52100 steel, respectively. Chemical analysis of an Al_2O_3 counterbody was performed using a Hitachi Tabletop TM3030Plus scanning electron microscope (SEM) equipped with energy-dispersive X-ray spectroscopy (EDS) at an accelerating voltage of 15 kV and a magnification of 150×. The structure and phases of the coating were analyzed with a Rigaku Ultima III X-ray diffractometer (XRD) with a Cu Kα X-ray source performed with a 1°/min scanning rate, 0.02° step increments, and in $\theta-2\theta$ scanning mode. Raman two-dimensional (2D) mapping was conducted with a Renishaw Raman microscope, a 532 nm edge laser, an exposure time of 2 s, and a spectral range of approximately 500−2200 cm^{-1}.

Transmission electron microscopy (TEM) and scanning TEM (STEM) analyses of the collected tribofilm debris were performed using a FEI Tecnai G2 F20 ST S-Twin equipped with a 200 kV Schottky field emission source. Similar analysis of focused ion beam (FIB) cross sections of the prepared coating was performed using a JEOL 2100F TEM. TEM cross sections were prepared by first depositing a Cr layer in a metal deposition chamber to protect the tribofilm from C deposition by electron beam in the FIB. A Pt layer was then deposited in the FIB to protect the cross section during thinning. The microscope is equipped with a Gatan OneView 4k × 4k digital camera, a model Continuum Gatan imaging filter (GIF), Gatan Digiscan II system, a Gatan 806 high-angle annular detector (HAADF), and an EDAX Octane Elite Super windowless silicon drift detector (SDD) X-ray energy-dispersive spectrometer (XEDS). The GIF can collect energy-filtered TEM (EFTEM) images and electron energy loss spectroscopy (EELS) with the low-loss and high-loss spectra being acquired simultaneously. All imaging and spectroscopy data was collected and analyzed using Gatan Microscopy Suite software version 3.5. XEDS and dual EELS spectrum images could be acquired simultaneously. The TEM samples were prepared by a standard in situ lift-out procedure using a Thermo Fisher Helios dual-beam FIB system utilizing AutoTEM 4 software, with the final thinning being done manually. Approximately three to five micrometer wide windows were cut with a frame at the bottom to prevent warping of the substrate when thinned.

To analyze the tribofilm with EELS, the Mo-M, N-K, and V-L edges from the coatings were used after correcting for plural scattering to create internal standards that were used to fit the data from the tribofilm. This allowed the edge overlaps with C, Ca, and O to be resolved. If a 0.3 eV dispersion was used, not all of the elements could be analyzed, but those that were not had low signals and were better detected with the XEDS system.

3. RESULTS AND DISCUSSION

The as-deposited MoVN-Cu coating was characterized with grazing-angle XRD (see Figure 1), confirming the presence of molybdenum, cubic δ-VN, and cubic γ-Mo_2N. The coating was deposited at 270 °C in a high-vacuum system by the direct current magnetron sputtering. The targets were pure Mo (99.95%), V (99.95%), and Cu (99.999%) deposited at the sputtering applied power of 9 W/cm^2 for Mo and V and 0.45 W/cm^2 for Cu. The targets were rotated during the deposition with an Ar/N_2 ratio of 130−55 sccm at 0.4 Pa total pressure. These coatings exhibited a consistent surface finish with an average surface roughness of 0.026 ± 0.006 μm. The Debye−Scherrer equation was used to calculate grain sizes of 7−8 nm within the nanocomposite coating structure. The STEM-BF (Figure 1g) and STEM-ADF (Figure 1h) imaging of the coating revealed a microstructure consistent with the calculated 7−8 nm grain size and columnar grain growth mechanisms. The coating hardness was measured to be 30.4 ± 4.1 GPa. TEM, XEDS, and principal component analysis (PCA) were used to reveal the nanocomposite coating morphology. The coating structure consists of modulating layers of vanadium and molybdenum (Figure 1c,d) with

https://doi.org/10.1021/acsami.3c01953
ACS Appl. Mater. Interfaces 2023, 15, 30070−30082

Table 1. Parameters of the Tribological Experiments Conducted on the MoVN-Cu Coating

experiment #	fuel	frequency (Hz)	average sliding velocity (mm/s)	temperature (°C)	initial contact pressure (GPa)
1	ethanol	25	25	25	0.82
2					1.11
3					1.25
4				50	0.82
5					1.11
6					1.25
7		50	50	25	0.82
8					1.11
9					1.25
10				50	0.82
11					1.11
12					1.25
13	dodecane	25	25	25	0.82
14					1.11
15					1.25
16				50	0.82
17					1.11
18					1.25
19		50	50	25	0.82
20					1.11
21					1.25
22				50	0.82
23					1.11
24					1.25

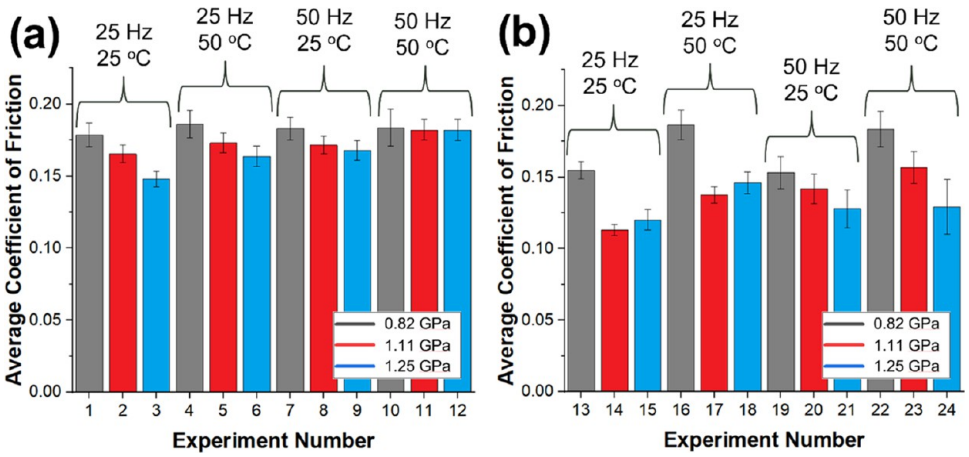

Figure 3. Comparison of the average coefficient of friction for experiments conducted on the MoVN-Cu coating in (a) ethanol and (b) dodecane fuel lubricants. These experiments were performed using MoVN-Cu-coated AISI 52100 steel flat surfaces, Al_2O_3 counterbodies (d = 6.00−6.35 mm), a stroke length of 1 mm, and a duration of 30 min.

nanoscale copper clusters (average size of 2−4 nm) disbursed throughout (Figure 1e).

Prior to the detailed tribological analysis of the MoVN-Cu coating, a comparison of the coating to a standard alloy used in heavy-duty fuel injection systems (AISI 52100 steel) was performed. As shown in Figure 2a, when subjected to identical tribological experiments, the MoVN-Cu coating provided a consistently lower and more stable coefficient of friction than the AISI 52100 steel. In addition, Figure 2b shows that the AISI 52100 steel experienced significantly more wear than the MoVN-Cu coating, which is further supported by the smaller wear scar dimensions for the MoVN-Cu coating as shown in Figure 2c,d. These results show the potential advantages of decreased friction and wear if the MoVN-Cu coating would be used to protect AISI 52100 steel fuel injection system components.

After the initial assessment, the coating was tested in a range of load, temperature, and sliding velocity conditions to evaluate its stability and consistency of the tribological behavior (Table 1).

Figure 3 presents the different conditions used in the experimental matrix. The variation of normal load (i.e., contact pressure) appears to have the most significant impact on the coefficient of friction. Although the differences in the coefficient of friction among the various experimental conditions were nominal, a trend toward higher coefficients of friction occurs for experiments with lower normal load is apparent (see Figure 3). Within the MoVN-Cu coating, the constituent nitride phases provide the coating with hardness

https://doi.org/10.1021/acsami.3c01953
ACS Appl. Mater. Interfaces 2023, 15, 30070−30082

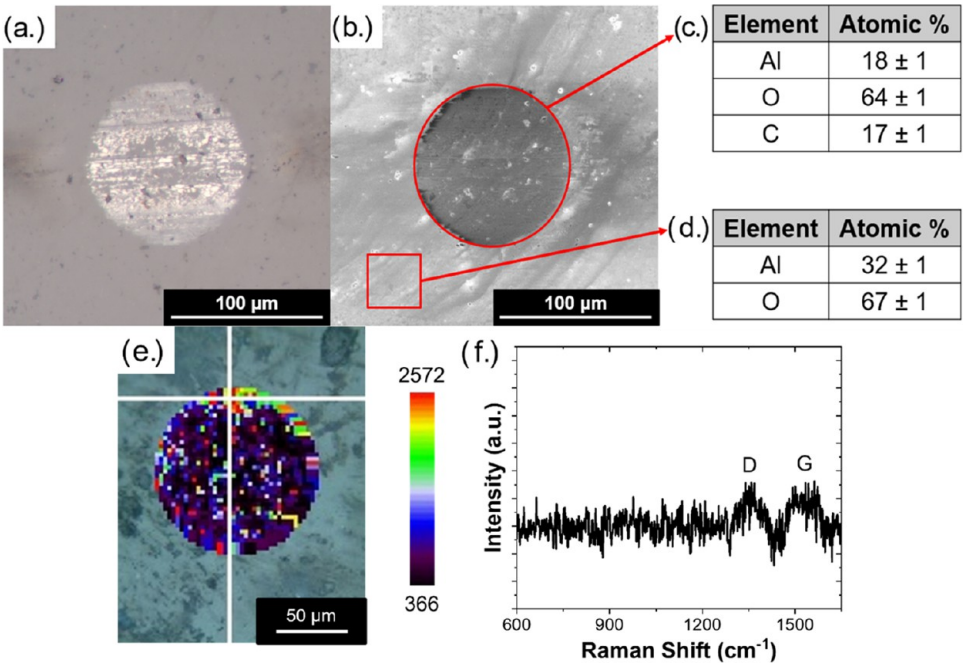

Figure 4. (a) Bright-field optical image of the wear scar left on the Al_2O_3 counterbody for experiment 24; (b) corresponding SEM BSE image of the wear scar; (c) analysis results of the EDS spectra for the worn surface showing the presence of a carbon-based tribofilm; (d) analysis results of the EDS spectra for the unworn surface; (e) selected area for Raman spectroscopy mapping of the D and G peak intensities, and (f) Raman spectra selected from within the wear scar area.

and wear resistance akin to other hard ceramic coatings, while the grains of copper provide a supply of the catalyst that facilitates the formation of the amorphous carbon tribofilm.[43] Therefore, a lower coefficient of friction when a higher normal load is used can be attributed to a greater amount of wear of the MoVN-Cu coating, thus exposing more copper surfaces and allowing for further generation of the low-COF amorphous carbon tribofilm. Relatively large coating wear rates provide an opportunity for the tribofilm to replenish within the wear track where the film had previously been pushed outside of the contact. This mechanism results in the lower observed coefficients of friction. A slight deviation in this trend is seen for the dodecane tests performed at 25 Hz, as the 1.11 GPa initial contact pressure experiments show nominally lower COF than the 1.25 GPa initial contact pressure experiments. Dodecane is a long-chain, high-surface-tension, and nonpolar molecule. As dodecane has higher surface tension than ethanol, this lubricant wets the sliding surfaces poorly and exhibits a decreased ability of liquid molecules to move freely past each other.[51] Ethanol, on the other hand, consists of short-chain, low-surface-tension, and polar molecules that can move past each other easily; thus, ethanol has a lower viscosity than dodecane.[52] Ethanol also has a lower pressure−viscosity coefficient than dodecane; therefore, the increase in viscosity under high loads is less pronounced for ethanol. The slight change in behavior for the experiments performed with dodecane at 25 Hz can be attributed to the increased pressure in the liquid lubricant film, providing greater separation between the two sliding surfaces and resulting in less predictable COF values.

The stability of the tribofilm was evaluated by analysis of the wear mark on the Al_2O_3 ball counterpart (Figure 4). Results indicate significant carbon presence in the form of wear debris. Notably, no coating material transfer is observed. Optical images of the formed wear tracks (Figure 5) indicated very minimal wear of the surfaces for further evaluation of the surface conditions.

To better understand the low-friction behavior of the MoVN-Cu coating versus Al_2O_3 sliding pair, the counterbody from experiment 24, which has the highest sliding speed and contact load (see Table 1 for details) was analyzed with EDS and Raman spectroscopy. As shown in Figure 4a,c, the EDS data from the center of the counterbody indicates the presence of carbon. On the other hand, EDS data collected from the outer edge of the counterbody lacks carbon, as shown in Figure 4b,d. The presence of carbon only on the contact surface indicates that, during sliding, the tribofilm that is formed between the MoVN-Cu coating and the Al_2O_3 counterbody readily adheres to both surfaces. Raman spectroscopy was performed on the Al_2O_3 counterbody wear scar, shown in Figure 4e,f. Though the detection of the Raman signal on the counterbody is complicated by the curvature of the substrate, the presence of the characteristic carbon D and G peaks (at 1340 and 1560 cm^{-1}, respectively) suggests the amorphous nature of carbon present in the wear area. This analysis is consistent with the following in-depth analysis of the tribofilm observed on the MoVN-Cu coating surface, which is discussed in more detail later. Thus, both the flat MoVN-Cu coating surface and the Al_2O_3 counterbody are protected by the easily sheared tribofilm, providing the low coefficient of friction values measured during sliding.

Figure 5 displays the wear scar dimensions of the MoVN-Cu flat specimens and Al_2O_3 balls produced with the experimental matrix to highlight the effect of each parameter on the tribological performance of the MoVN-Cu coating. As shown in Figure 3, the coefficient of the friction range is relatively small with each experiment having a COF from 0.15−0.20. As shown in Figure 5a,b, alterations of the reciprocating frequency and temperature had a nominal effect on the wear scar dimensions. On the other hand, the initial contact pressure had

https://doi.org/10.1021/acsami.3c01953
ACS Appl. Mater. Interfaces 2023, 15, 30070−30082

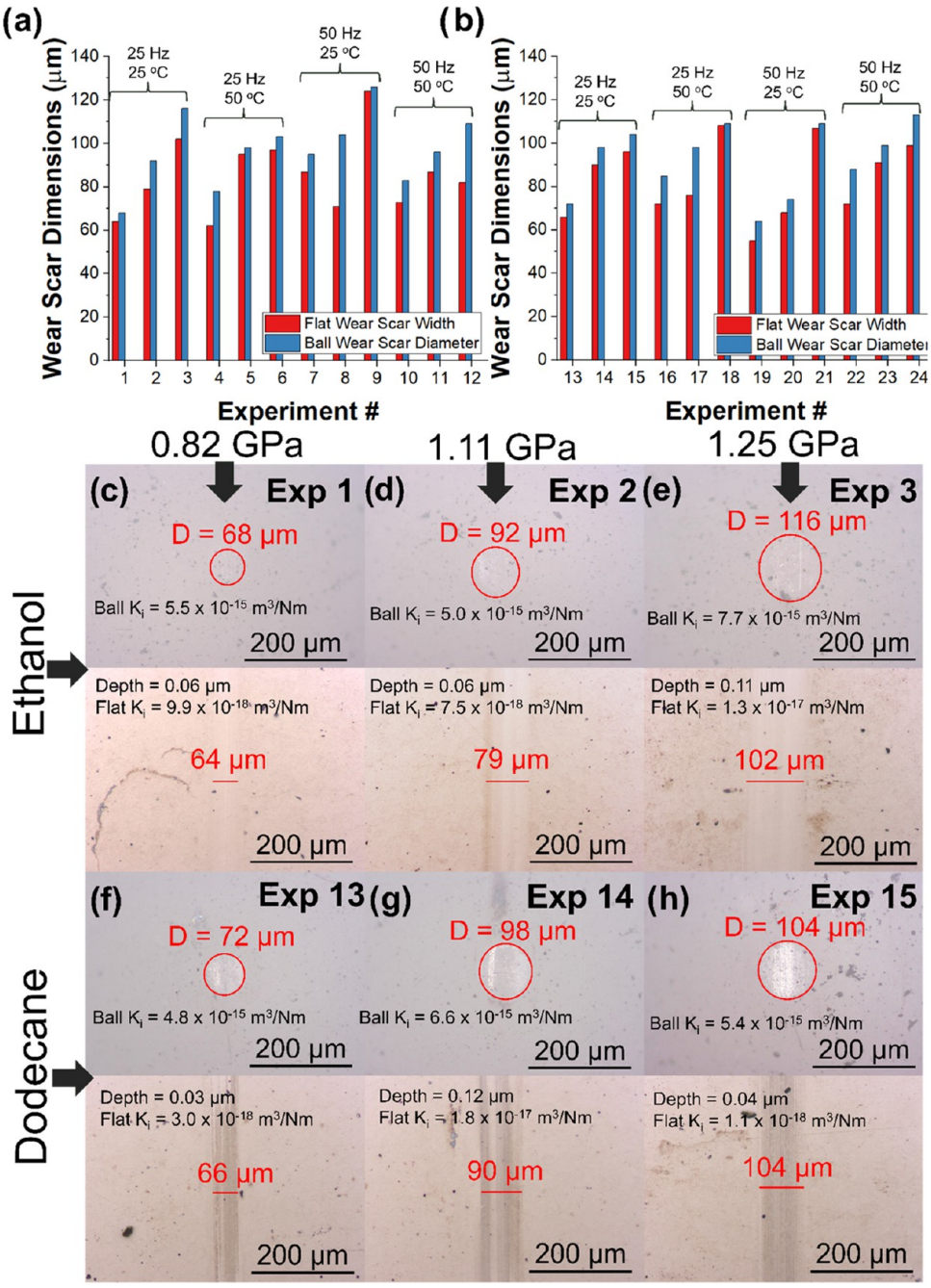

Figure 5. Wear scar dimensions of the flat and ball specimens for (a) experiments 1−12 performed with ethanol and (b) experiments 13−24 performed with dodecane. (c−h) Optical images of the wear scars on the Al_2O_3 counterbodies (top) and MoVN-Cu coating surfaces (bottom) for the experiments conducted at 25 °C and with a 25 Hz reciprocating frequency.

significant influence on the wear scar dimensions. To highlight the effect of initial contact pressure, the optical microscopy images of the MoVN-Cu and Al_2O_3 worn surfaces for the experiments conducted at 25 °C and 25 Hz are presented in Figure 5c−h. The relative size of the worn surfaces increased with increasing initial contact pressure due to more wear of the coating surface. In addition, comparing Figure 5c−e and 5f−h indicates that the wear of the materials is diminished when the surfaces were lubricated with dodecane, as opposed to the lower-viscosity ethanol lubrication. Figure 5c−h also displays the wear scar depths and specific wear rates for the sliding pairs. Due to the dynamic tribocatalytic process of simultaneous material growth and removal, these wear metrics provide uncertainties for characterization; therefore, the wear scar dimensions are provided for discussion as well. Regardless of the sliding contact conditions, the overall performance of the MoVN-Cu film is dictated by the competition between two mechanisms, i.e., the replenishment of the generated tribofilm and the wear of the coating material.

The change in mechanical properties across the surface of the wear tracks left on a representative experiment on MoVN-Cu coating and AISI 52100 steel was analyzed using nanoindentation, as shown in Figure 6. Mapping of the MoVN-Cu surface revealed that the hardness and modulus of the coating decreased from 30.4 and 347.2 GPa of the unworn surface to approximately 25 and 300 GPa for the worn surface,

https://doi.org/10.1021/acsami.3c01953
ACS Appl. Mater. Interfaces 2023, 15, 30070−30082

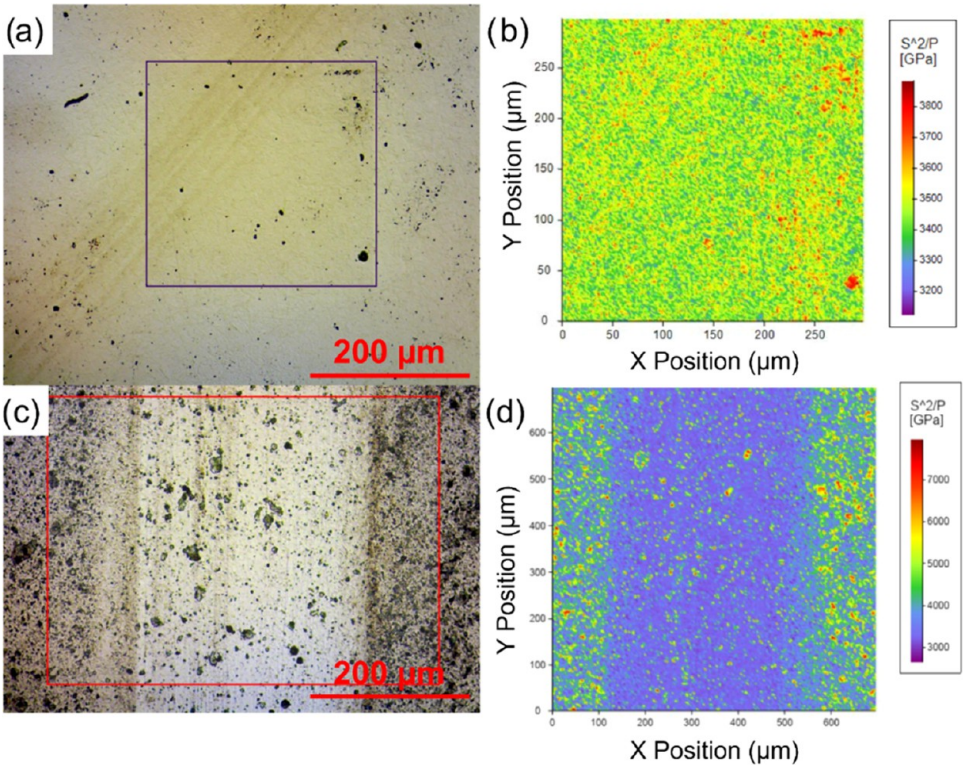

Figure 6. Optical microscopy and nanoindentation mapping of stiffness squared over load for the wear tracks left on the flat surfaces of (a, b) MoVN-Cu coating and (c, d) AISI 52100 steel.

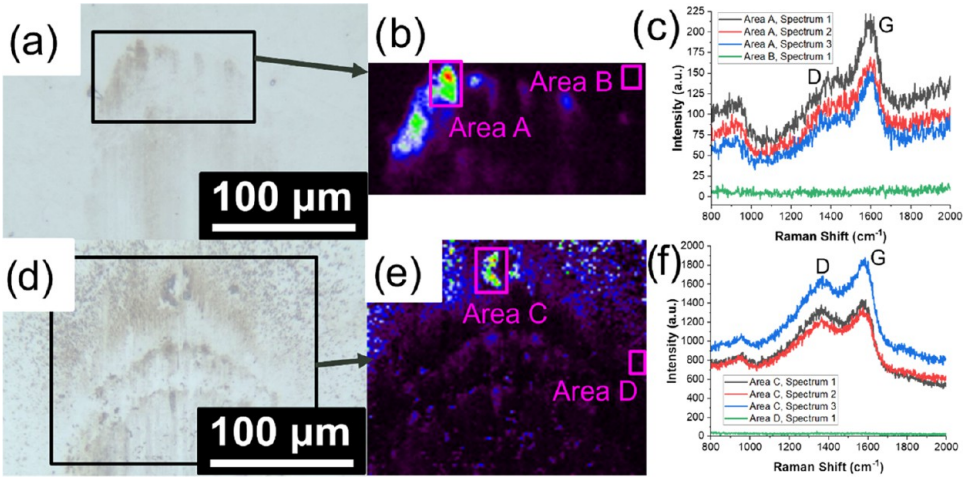

Figure 7. Optical images of the wear scar end on the MoVN-Cu coating for experiment 11 in ethanol (a) and experiment 24 in dodecane (d), selected areas for Raman spectroscopy mapping of the G peak intensity for experiment 11 (b) and experiment 24 (e). Three high-intensity spectra were selected from areas A and C, which are covered by the tribofilm and one low-intensity spectrum was selected from areas B and D, which are significantly outside of the mechanical contact and are shown in panel (c) for experiment 11 and (f) for experiment 24. Experiments 11 and 24 were conducted with 50 Hz reciprocating frequencies, a temperature of 50 °C, and 1.11 and 1.25 GPa initial contact pressures, respectively.

respectively. The morphology and surface roughness of the worn steel surface inhibited extracting of hardness and modulus values for the steel. Therefore, to compare the MoVN-Cu and AISI 52100 steel surfaces, mapping of the worn surfaces of both materials were generated using stiffness values (S^2/P) to eliminate the effect of surface roughness. For both the steel and coating surfaces, the majority of indentations revealed S^2/P values from 3000−4000 GPa. Although the MoVN-Cu coating contains hard ceramic particles which provide wear resistance, the mechanical properties of thin films are highly influenced by the properties of the substrate material the film is adhered to, particularly in terms of stiffness properties.[53] As the MoVN-Cu coating is only 600 nm in thickness, its mechanical properties mirror that of the AISI 52100 steel that the coating was deposited onto.[19] There is, however, a contrast between the coating and steel mechanical properties in terms of the gradient of values present. As shown in Figure 6d, there are regions of the AISI 52100 steel surface, particularly outside of the wear track on the unworn surface, which indicate S^2/P values exceeding 7000 GPa, whereas the MoVN-Cu surface shown in Figure 6b maintains values in the range of 3000−4000 GPa. During the sliding process, there is

https://doi.org/10.1021/acsami.3c01953
ACS Appl. Mater. Interfaces 2023, 15, 30070−30082

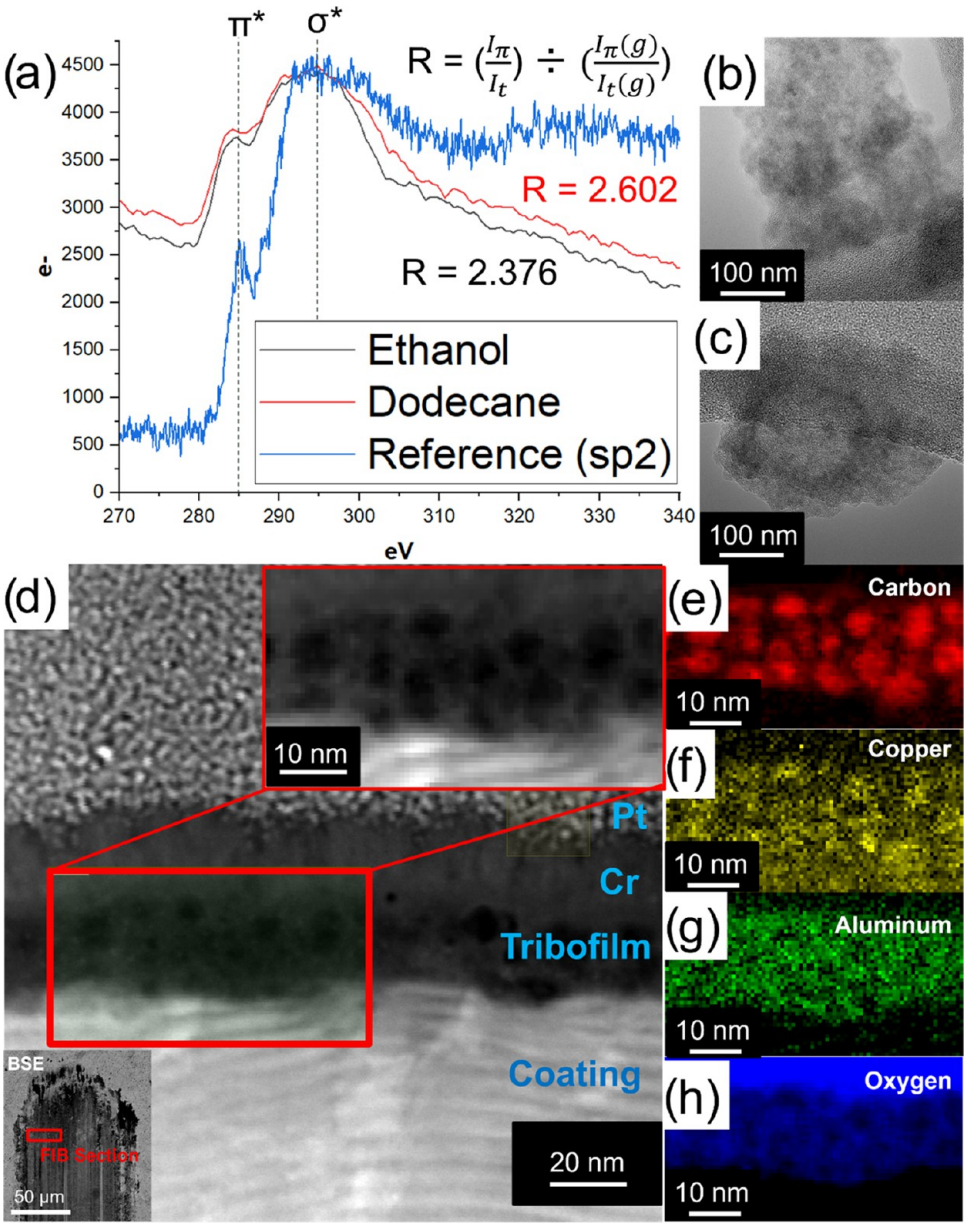

Figure 8. STEM analysis of tribofilm particles formed on the MoVN-Cu coating surface during tribological experiments; (a) EELS spectra for the tribofilm particles formed on the MoVN-Cu surface in ethanol and dodecane fuel environments and a reference sp^2 spectra; (b) HRTEM image of the tribofilm particle generated during the experiment in ethanol; (c) HRTEM image of the tribofilm particle generated during the experiment in dodecane; (d) HAADF image of the tribofilm produced in a dodecane environment and adhered to the coating surface with the corresponding normalized EELS map of (e) carbon, XEDS map of (f) copper and (g) aluminum, and normalized EELS map of (h) oxygen. The lower left inset image of panel (d) is a BSE image of the wear track from which the FIB section was collected for TEM analysis.

deformation of the load-bearing asperities and localized heating of contacting surfaces. For many metals, including AISI 52100 steel, these contacting surfaces can harden via several mechanisms. One is the refinement of the metal grains at and below the worn surface. During wear, the strains imposed on the metallic surface result in the generation and migration of dislocations, which in addition to frictional heating can lead to recrystallization of the near-surface material into a finer grain structure.[54] These finer grains produce a work-hardened layer of the metal, described by the Hall−Petch relationship.[54−56] A second mechanism by which metal surfaces harden during wear is surface oxidation and mechanical mixing. Aided by the strain and heating associated with sliding, metallic surfaces can oxidize readily and form brittle oxide particles on the surface. Subsequent wear of this oxide layer can incorporate oxide particles within the metal, providing a mechanically mixed composite of metal grains and oxide particles, which is supported by the underlying refined metal grains.[54,56−58] In contrast, ceramic materials which have limited ability to generate and flow dislocations, such as the predominant phases of the MoVN-Cu coating, experience less change in their mechanical properties at the worn surface.[54] Therefore, the MoVN-Cu surface maintains more consistent stiffness across the worn and nonworn surfaces. This can be attributed to the protection of the surface via the production of the carbon-rich tribofilm and the superior wear-resistance properties of the ceramic constituents within the nanocomposite structure.

https://doi.org/10.1021/acsami.3c01953
ACS Appl. Mater. Interfaces 2023, 15, 30070−30082

To confirm the carbon-rich nature of the tribofilms and the mechanisms responsible for the beneficial tribological performance, representative wear tracks formed in ethanol and dodecane were evaluated using Raman spectroscopy (Figure 7).

Results of the Raman analysis indicate the characteristic carbon disorder mode (D) and graphitic in-plane mode (G) peaks at approximately 1340 and 1560 cm^{-1}, respectively. The appearance of the D and G peaks indicate that the carbon-rich film exhibits the structure of amorphous carbon, which is well documented to provide low friction during sliding.[19] The irregularities in intensities of the D and G peaks are attributed to the nonuniformity of the tribofilm coverage on the MoVN-Cu surface. However, the tribofilms surrounding the wear tracks produced under dodecane lubrication provided substantially greater intensities of the characteristic carbon peaks, indicating that dodecane lubrication supports increased amorphous carbon film-formation abilities compared to ethanol.[43]

Scanning transmission electron microscopy (STEM) and electron energy loss spectroscopy were performed on the wear debris produced during tribological experiments to determine the predominant interatomic local bonding arrangements of the carbon-rich tribofilms (Figure 8). To collect the debris generated in both fuel environments, a scalpel was used to scrape off some of the tribofilm deposited at the ends of the wear scars for experiments conducted in ethanol (experiments 16 and 24) and dodecane (experiment 11); the debris was then collected on TEM grids and analyzed. In addition, one FIB cross section of a worn coating surface was prepared for TEM analysis. In EELS spectra, the peak preceding the carbon K-edge peak is representative of only the sp^2-bonded electrons. By comparing the areas of the prepeak of the collected tribofilm debris to a completely sp^2-bonded reference, the sp^2 ratio for the debris can be calculated according to the following formula

$$R = \left(\frac{I_\pi}{I_t}\right)/\left(\frac{I_\pi(g)}{I_t(g)}\right)$$

where I_π and $I_\pi(g)$ are the intensity of the prepeak and I_t and $I_t(g)$ are the intensity of the π^* and s peaks integrated over a range of 50 eV for the analyzed sample and sp^2 reference, respectively.[59] The sp^2 reference used was produced from an amorphous carbon film sputtered in vacuum at room temperature.[59]

HRTEM images of the debris produced during sliding are shown in Figure 8b for ethanol lubrication and in Figure 8c for dodecane lubrication. As shown in Figure 8a, the debris produced in ethanol and dodecane shows apparent π^* peaks at 285 eV, indicating that the tribofilm is amorphous and contains sp^2-bonded graphitic carbon, which can provide a low-friction easily sheared film between the coating surface and counterbody. Calculating the ratio of sp^2 to sp^3 bonding revealed that the tribofilm generated in ethanol and dodecane were 70 and 72% sp^2-bonded, respectively. A FIB section was collected from a tribofilm-covered area of the worn MoVN-Cu surface of one of the tribological experiments such that the tribofilm could be analyzed (see the inset of Figure 8d). Elemental analysis of the tribofilm adhered to the coating surface in the FIB sample indicates the presence of copper, carbon, aluminum, and oxygen (see Figure 8d–h). The observation of aluminum and oxygen is attributed to the transfer of the wear debris produced from the Al_2O_3 counterbodies. Tribocatalytic reactions may occur for systems which have available catalytically active surfaces, a source of carbon, and thermomechanical energy for the activation of dehydrogenation and random scission of the C–C bonds in the carbon source.[26,28] Initially, the hydrocarbon molecules are homogeneously distributed over the MoVN-Cu surface. When sliding is initiated on the Cu surface, the hydrocarbon molecules degrade via two competing processes. First, the C–H bonds of the hydrocarbon dissociate, aided by the catalytic metal surface, producing dehydrogenated chains. Second, random scission of the backbone C–C bonds occurs, which forms shorter hydrocarbon fragments. These short hydrocarbon fragments recombine at the interface to form a graphitic tribofilm. The free hydrogen produced from the dehydrogenation of the hydrocarbon may adsorb and diffuse into the metal surface or recombine at the material interface to form H_2 molecules.[28] The apparent correlation between copper-rich and carbon-rich areas within the tribofilm reinforce that the copper clusters provided the catalytic surface, which facilitates the formation of the carbon-rich film. Previous studies of the MeN-Cu coatings justified the tribofilm formation by simulating the mechanism on Cu surfaces within the coating but did not have a practical demonstration of this phenomenon. In this work, we demonstrate with TEM analysis that the carbon is correlated with the Cu inclusions, verifying that the Cu surfaces provide the catalytic surface for tribofilm formation. The ability of the hard MoVN-Cu coating to catalytically transform components of the hydrocarbon environment (ethanol or dodecane molecules) provided this material a unique response to tribologically induced stresses. For an unprotected steel surface in a low-viscosity hydrocarbon environment, material wear and subsurface deformations made the steel alloy vulnerable to gross surface damage such as scuffing;[60] however, the MoVN-Cu coating uses such conditions of elevated temperature and shear stresses to promote the generation of a friction-reducing carbon tribofilm that effectively protects the underlying steel surface under a wide variety of tribological contact conditions.

4. CONCLUSIONS

The tribological performance of the MoVN-Cu tribocatalytic coatings was evaluated under a wide range of experimental conditions. These MoVN-Cu coatings were found to provide an adaptive tribological performance due to the inclusion of catalytically active copper clusters within the nanocomposite structure. TEM and Raman spectroscopy were used to confirm the amorphous carbon nature of the tribofilms with predominantly graphite-like interatomic bonding arrangements generated during the wear of the MoVN-Cu material. TEM analysis also demonstrated the correlation between the Cu within the coating and the C-rich tribofilm formed, indicating that the Cu surfaces within the coating provide the catalytic centers for the tribofilm formation. The presence of this catalytically formed graphitic character transfer film was linked to lower coefficients of friction and substantially less wear of the MoVN-Cu coating when compared to uncoated AISI 52100 steel when tested under identical contact conditions. The MoVN-Cu tribological performance showed consistent low-friction and low-wear behavior under varying operating temperatures (25–50 °C) and reciprocating frequencies (25–50 Hz). Tribofilm formation was observed in the presence of both ethanol and dodecane and was more pronounced in the

https://doi.org/10.1021/acsami.3c01953
ACS Appl. Mater. Interfaces 2023, 15, 30070–30082

dodecane environment. The MoVN-Cu coating was notably adaptive in its tribological response under different normal loads (initial maximum contact pressures of 0.82−1.25 GPa). The coefficient of friction during experiments was minimal when the initial contact pressure was at its maximum values, which is attributed to the increased generation of the low-friction tribofilm. The well-established wear resistance and load support characteristics intrinsic to hard nitride coatings in combination with the novel adaptive catalytic tribofilm lubrication mechanism characteristic of the MoVN-Cu coating explored here provides a new approach for improving the wear endurance and performance of mechanical components handling low-viscosity fuels. This approach has the potential for considerably improving the lifetime of components within the fuel injection systems of emerging combustion engines, tailored for more environmentally benign low-viscosity hydrocarbon fuels.

AUTHOR INFORMATION

Corresponding Authors

Andrey A. Voevodin − *Department of Materials Science and Engineering, University of North Texas, Denton, Texas 76203, United States*; Phone: 940.565.4324; Email: Andrey.Voevodin@unt.edu

Samir Aouadi − *Department of Materials Science and Engineering, University of North Texas, Denton, Texas 76203, United States*; Phone: 940.565.4759; Email: Samir.Aouadi@unt.edu

Diana Berman − *Department of Materials Science and Engineering, University of North Texas, Denton, Texas 76203, United States*; orcid.org/0000-0002-9320-9772; Phone: 940.891.6778; Email: Diana.Berman@unt.edu

Authors

Kelly Jacques − *Department of Materials Science and Engineering, University of North Texas, Denton, Texas 76203, United States*; orcid.org/0000-0002-4005-421X

Asghar Shirani − *Department of Materials Science and Engineering, University of North Texas, Denton, Texas 76203, United States*

Jesse Smith − *Department of Materials Science and Engineering, University of North Texas, Denton, Texas 76203, United States*

Thomas W. Scharf − *Department of Materials Science and Engineering, University of North Texas, Denton, Texas 76203, United States; Army Research Directorate, U.S. DEVCOM Army Research Laboratory, Aberdeen Proving Ground, Maryland 21005, United States*

Scott D. Walck − *SURVICE Engineering, Inc. DEVCOM Army Research Laboratory, Aberdeen Proving Ground, Maryland 21005, United States*

Stephen Berkebile − *Army Research Directorate, U.S. DEVCOM Army Research Laboratory, Aberdeen Proving Ground, Maryland 21005, United States*

Osman Levent Eryilmaz − *Applied Materials Division, Argonne National Laboratory, Lemont, Illinois 60439, United States*; orcid.org/0000-0002-7515-3242

Complete contact information is available at: https://pubs.acs.org/10.1021/acsami.3c01953

Notes

The authors declare no competing financial interest.

ACKNOWLEDGMENTS

Research was sponsored by the Army Research Laboratory and was accomplished under Cooperative Agreement Number W911NF-20-2-0198. The authors acknowledge partial support from the National Science Foundation (NSF) (Award No. 2018132). Work at Argonne National Laboratory was supported by the U.S. Department of Energy, Office of Energy Efficiency and Renewable Energy, Vehicle Technologies and Advanced Manufacturing Offices under Contract DE-AC02-06CH11357. The research reported in this document was performed in connection with contract/instrument W15P7T-19-D-0126 with the DEVCOM Army Research Laboratory. The views and conclusions contained in this document are those of the authors and should not be interpreted as representing the official policies, either expressed or implied, of the Army Research Laboratory or the U.S. Government. The U.S. Government is authorized to reproduce and distribute reprints for Government purposes notwithstanding any copyright notation herein. The characterization work was performed in part at the University of North Texas' Materials Research Facility.

REFERENCES

(1) Qu, J.; Truhan, J. J.; Blau, P. J.; Meyer, H. M., III Scuffing Transition Diagrams for Heavy Duty Diesel Fuel Injector Materials in Ultra Low-Sulfur Fuel-Lubricated Environment. *Wear* **2005**, *259*, 1031−1040.

(2) Ayyagari, A.; Alam, K. I.; Berman, D.; Erdemir, A. Progress in Superlubricity Across Different Media and Material Systems - A Review. *Front. Mech. Eng.* **2022**, *8*, No. 908497.

(3) Jääskeläinen, H. Fuel Property Testing: Lubricity. DieselNet, 2008. Retrieved April 20, 2023, from https://dieselnet.com/tech/fuel_diesel_lubricity.php.

(4) Marian, M.; Berman, D.; Rota, A.; Jackson, R. L.; Rosenkranz, A. Layered 2D Nanomaterials to Tailor Friction and Wear in Machine Elements—A Review. *Adv. Mater. Interfaces* **2022**, *9*, No. 2101622.

(5) Hogmark, S.; Jacobson, S.; Larsson, M. Design and Evaluation of Tribological Coatings. *Wear* **2000**, *246*, 20−33.

(6) Arkoudeas, P.; Karonis, D.; Zannikos, F.; Lois, E. Lubricity Assessment of Gasoline Fuels. *Fuel Process. Technol.* **2014**, *122*, 107−119.

(7) Hsieh, P. Y.; Bruno, T. J. A Perspective on the Origin of Lubricity in Petroleum Distillate Motor Fuels. *Fuel Process. Technol.* **2015**, *129*, 52−60.

(8) Naegeli, D. W.; Lacey, P. I.; Alger, M. J.; Endicott, D. L. In *Surface Corrosion in Ethanol Fuel Pumps*, SAE Transactions 1997; pp 564−571.

(9) Berman, D.; Erdemir, A.; Sumant, A. V. Approaches for Achieving Superlubricity in Two-Dimensional Materials. *ACS Nano* **2018**, *12*, 2122−2137.

(10) Shirani, A.; Hu, Q.; Su, Y.; Joy, T.; Zhu, D.; Berman, D. Combined Tribological and Bactericidal Effect of Nanodiamonds as Potential Lubricant for Artificial Joints. *ACS Appl. Mater. Interfaces* **2019**, *11*, 43500−43508.

(11) Shirani, A.; Nunn, N.; Shenderova, O.; Osawa, E.; Berman, D. Nanodiamonds for Improving Lubrication of Titanium Surfaces in Simulated Body Fluid. *Carbon* **2019**, *143*, 890−896.

(12) Zhai, W.; Srikanth, N.; Kong, L. B.; Zhou, K. Carbon Nanomaterials in Tribology. *Carbon* **2017**, *119*, 150−171.

(13) Robertson, J. Properties of Diamond-Like Carbon. *Surf. Coat. Technol.* **1992**, *50*, 185−203.

(14) Donnet, C.; Erdemir, A. *Tribology of Diamond-Like Carbon Films: Fundamentals and Applications*; Springer Science & Business Media, 2007.

(15) Erdemir, A.; Martin, J. M. Superior Wear Resistance of Diamond and DLC Coatings. *Curr. Opin. Solid State Mater. Sci.* **2018**, *22*, 243−254.
(16) Lawes, S. D. A.; Fitzpatrick, M.; Hainsworth, S. V. Evaluation of the Tribological Properties of DLC for Engine Applications. *J. Phys. D: Appl. Phys.* **2007**, *40*, 5427.
(17) Mutafov, P.; Lanigan, J.; Neville, A.; Cavaleiro, A.; Polcar, T. DLC-W Coatings Tested in Combustion Engine—Frictional and Wear Analysis. *Surf. Coat. Technol.* **2014**, *260*, 284−289.
(18) Van der Kolk, G. Wear Resistance of Amorphous DLC and Metal Containing DLC in Industrial Applications. In *Tribology of Diamond-Like Carbon Films*; Springer, 2008; pp 484−493.
(19) Ajayi, O. O.; Alzoubi, M.; Erdemir, A.; Fenske, G. Effect of Carbon Coating on Scuffing Performance in Diesel Fuels. *Tribol. Trans.* **2001**, *44*, 298−304.
(20) Bhowmick, S.; Yang, Z.; Banerji, A.; Alpas, A. T. Effect of Graphene Nanoplates Dispersed in Ethanol on Frictional Behaviour of Tool Steel Running Against Uncoated and DLC-Coated Tool Steel. *Tribol. Lett.* **2019**, *67*, No. 32.
(21) Treutler, C. P. Industrial Use of Plasma-Deposited Coatings for Components of Automotive Fuel Injection Systems. *Surf. Coat. Technol.* **2005**, *200*, 1969−1975.
(22) Hershberger, J.; Öztürk, O.; Ajayi, O. O.; Woodford, J. B.; Erdemir, A.; Erck, R. A.; Fenske, G. R. Evaluation of DLC Coatings for Spark-Ignited, Direct-Injected Fuel Systems. *Surf. Coat. Technol.* **2004**, *179*, 237−244.
(23) Radi, P. A.; Vieira, A.; Manfroi, L.; Nass, K. C.; Ramos, M. A.; Leite, P.; Martins, G. V.; Jofre, J. B.; Vieira, L. Tribocorrosion and Corrosion Behavior of Stainless Steel Coated with DLC Films in Ethanol with Different Concentrations of Water. *Ceram. Int.* **2019**, *45*, 9686−9693.
(24) Rübig, B.; Heim, D.; Forsich, C.; Dipolt, C.; Mueller, T.; Gebeshuber, A.; Kullmer, R.; Holecek, R.; Lugmair, C.; Krawinkler, M.; Strobl, V. Tribological Behavior of Thick DLC Coatings Under Lubricated Conditions. *Surf. Coat. Technol.* **2017**, *314*, 13−17.
(25) Masuko, M.; Kudo, T.; Suzuki, A. Effect of Surface Roughening of Substrate Steel on the Improvement of Delamination Strength and Tribological Behavior of Hydrogenated Amorphous Carbon Coating Under Lubricated Conditions. *Tribol. Lett.* **2013**, *51*, 181−190.
(26) Berman, D.; Erdemir, A. Achieving Ultralow Friction and Wear by Tribocatalysis: Enabled by In-Operando Formation of Nanocarbon Films. *ACS Nano* **2021**, *15*, 18865−18879.
(27) Ta, T. D.; Tieu, A. K.; Tran, B. H. Influences of Iron and Iron Oxides on Ultra-Thin Carbon-Based Tribofilm Lubrication. *Tribol. Int.* **2022**, No. 107665.
(28) Erdemir, A.; Ramirez, G.; Eryilmaz, O. L.; Narayanan, B.; Liao, Y.; Kamath, G.; Sankaranarayanan, S. K. R. S. Carbon-Based Tribofilms from Lubricating Oils. *Nature* **2016**, *536*, 67−71.
(29) Shirani, A.; Berkebile, S.; Berman, D. Promoted High-Temperature Lubrication and Surface Activity of Polyolester Lubricant with Added Phosphonium Ionic Liquid. *Tribol. Int.* **2023**, *180*, No. 108287.
(30) David Phillips, W.; Milne, N.Ashless Phosphorus−Containing Lubricating Oil Additives. In *Lubricant Additives*; CRC Press, 2017; pp 157−196.
(31) Luiz, J. F.; Spikes, H. Tribofilm Formation, Friction and Wear-Reducing Properties of Some Phosphorus-Containing Antiwear Additives. *Tribol. Lett.* **2020**, *68*, No. 75.
(32) Kajdas, C.; Hiratsuka, K. Tribochemistry, Tribocatalysis, and the Negative-Ion-Radical Action Mechanism. *Proc. Inst. Mech. Eng., Part J* **2009**, *223*, 827−848.
(33) Wang, B.; Chang, Q. Y.; Gao, K.; Fang, H. R.; Qing, T.; Zhou, N. N. The Synthesis of Magnesium Silicate Hydroxide with Different Morphologies and the Comparison of Their Tribological Properties. *Tribol. Int.* **2018**, *119*, 672−679.
(34) Chang, Q.; Rudenko, P.; Miller, D. J.; Wen, J.; Berman, D.; Zhang, Y.; Arey, B.; Zhu, Z.; Erdemir, A. Operando Formation of an Ultra-Low Friction Boundary Film from Synthetic Magnesium Silicon Hydroxide Additive. *Tribol. Int.* **2017**, *110*, 35−40.
(35) Kajdas, C.; Kulczycki, A.; Ozimina, D. A New Concept of the Mechanism of Tribocatalytic Reactions Induced by Mechanical Forces. *Tribol. Int.* **2017**, *107*, 144−151.
(36) Hiratsuka, K. I.; Kajdas, C.; Kulczycki, A.; Dante, R. C.*Tribocatalysis, Tribocatalysis, Tribochemistry, and Tribocorrosion*; Jenny Stanford Publishing, 2018; pp 163−255.
(37) Argibay, N.; Babuska, T. F.; Curry, J. F.; Dugger, M. T.; Lu, P.; Adams, D. P.; Nation, B. L.; Doyle, B. L.; Pham, M.; Pimentel, A.; Mowry, C.; Hinkle, A. R.; Chandross, M. In-Situ Tribochemical Formation of Self-Lubricating Diamond-Like Carbon Films. *Carbon* **2018**, *138*, 61−68.
(38) Curry, J. F.; Babuska, T. F.; Furnish, T. A.; Lu, P.; Adams, D. P.; Kustas, A. B.; Nation, B. L.; Dugger, M. T.; Chandross, M.; Clark, B. G.; et al. Achieving Ultralow Wear with Stable Nanocrystalline Metals. *Adv. Mater.* **2018**, *30*, No. 1802026.
(39) Shirani, A.; Li, Y.; Smith, J.; Curry, J.; Lu, P.; Wilson, M.; Chandross, M.; Argibay, N.; Berman, D. Mechanochemically Driven Formation of Protective Carbon Films from Ethanol Environment. *Mater. Today Chem.* **2022**, *26*, No. 101112.
(40) Ramirez, G.; Eryilmaz, O. L.; Fatti, G.; Righi, M. C.; Wen, J.; Erdemir, A. Tribochemical Conversion of Methane to Graphene and Other Carbon Nanostructures: Implications for Friction and Wear. *ACS Appl. Nano Mater.* **2020**, *3*, 8060−8067.
(41) Berman, D.; Mutyala, K. C.; Srinivasan, S.; Sankaranarayanan, S. K. R. S.; Erdemir, A.; Shevchenko, E. V.; Sumant, A. V. Iron-Nanoparticle Driven Tribochemistry Leading to Superlubric Sliding Interfaces. *Adv. Mater. Interfaces* **2019**, *6*, No. 1901416.
(42) Gao, K.; Wang, B.; Shirani, A.; Chang, Q.; Berman, D. Macroscale Superlubricity accomplished by Sb2O3-MSH/C Under High Temperature. *Front. Chem.* **2021**, *9*, No. 667878.
(43) Shirani, A.; Li, Y.; Eryilmaz, O. L.; Berman, D. Tribocatalytically-Activated Formation of Protective Friction and Wear Reducing Carbon Coatings from Alkane Environment. *Sci. Rep.* **2021**, *11*, No. 20643.
(44) Subramanian, C.; Strafford, K. N. Review of Multicomponent and Multilayer Coatings for Tribological Applications. *Wear* **1993**, *165*, 85−95.
(45) Walsh, F. C.; Ponce de Leon, C. A Review of the Electrodeposition of Metal Matrix Composite Coatings by Inclusion of Particles in a Metal Layer: an Established and Diversifying Technology. *Trans. IMF* **2014**, *92*, 83−98.
(46) Aouadi, S. M.; Luster, B.; Kohli, P.; Muratore, C.; Voevodin, A. A. Progress in the Development of Adaptive Nitride-Based Coatings for High Temperature Tribological Applications. *Surf. Coat. Technol.* **2009**, *204*, 962−968.
(47) Qu, J.; Truhan, J.; Blau, P. Detecting the Onset of Localized Scuffing in a Pin-on-Twin Fuel-Lubricated Test for Heavy-Duty Diesel Fuel Injectors. *Int. J. Engine Res.* **2005**, *6*, 1−9.
(48) Sivaramprasad, G.; Rao, M. V.; Prasad, D. Density and Viscosity of Ethanolv+ 1, 2-Dichloroethane, Ethanol + 1, 1, 1-Trichloroethane, and Ethanol + 1, 1, 2, 2-Tetrachloroethane Binary Mixtures. *J. Chem. Eng. Data* **1990**, *35*, 122−124.
(49) Caudwell, D. R.; Trusler, J.; Vesovic, V.; Wakeham, W. The Viscosity and Density of n-Dodecane and n-Octadecane at Pressures up to 200 MPa and Temperatures up to 473 K. *Int. J. Thermophys.* **2004**, *25*, 1339−1352.
(50) Moldoveanu, S.The Chemistry of the Pyrolytic Process. In *Techniques and Instrumentation in Analytical Chemistry*; Elsevier, 2010; Vol. *28*, pp 7−48.
(51) Koller, T. M.; Klein, T.; Giraudet, C. D.; Chen, J.; Kalantar, A.; Van der Laan, G. P.; Rausch, M. H.; Fröba, A. P. Liquid Viscosity and Surface Tension of n-Dodecane, n-Octacosane, Their Mixtures, and a Wax Between 323 and 573 K by Surface Light Scattering. *J. Chem. Eng. Data* **2017**, *62*, 3319−3333.
(52) Vazquez, G.; Alvarez, E.; Navaza, J. M. Surface Tension of Alcohol Water + Water from 20 to 50. Degree. C. *J. Chem. Eng. Data* **1995**, *40*, 611−614.

https://doi.org/10.1021/acsami.3c01953
ACS Appl. Mater. Interfaces 2023, 15, 30070−30082

(53) Zak, S.; Trost, C.; Kreiml, P.; Cordill, M. Accurate Measurement of Thin Film Mechanical Properties Using Nano-indentation. *J. Mater. Res.* **2022**, *37*, 1373−1389.
(54) Rainforth, W. M. Microstructural Evolution at the Worn Surface: A Comparison of Metals and Ceramics. *Wear* **2000**, *245*, 162−177.
(55) Sundström, A.; Rendón, J.; Olsson, M. Wear Behaviour of Some Low Alloyed Steels Under Combined Impact/Abrasion Contact Conditions. *Wear* **2001**, *250*, 744−754.
(56) Liu, Y.; Liskiewicz, T. W.; Beake, B. D. Dynamic Changes of Mechanical Properties Induced by Friction in the Archard Wear Model. *Wear* **2019**, *428*−*429*, 366−375.
(57) Blau, P. J.; Qu, J.; Truhan, J. J., Jr. *A Multi-Stage Model for Scuffing of Reciprocating Components with Special Consideration of Fuel Injector Plungers*; Oak Ridge National Lab. (ORNL): Oak Ridge, TN (United States), 2005.
(58) Hardell, J.; Hernandez, S.; Mozgovoy, S.; Pelcastre, L.; Courbon, C.; Prakash, B. Effect of Oxide Layers and Near Surface Transformations on Friction and Wear During Tool Steel and Boron Steel Interaction at High Temperatures. *Wear* **2015**, *330*−*331*, 223−229.
(59) Wan, L.; Egerton, R. Preparation and Characterization of Carbon Nitride Thin Films. *Thin Solid Films* **1996**, *279*, 34−42.
(60) Jacques, K.; Murthy, N.; Dixit, S.; Berman, D.; Berkebile, S. Method for Tribological Experiment to Study Scuffing Initiation on AISI 52100 Steel and Hard Ceramic Coatings. *Tribol. Int.* **2021**, *160*, No. 107001.

https://doi.org/10.1021/acsami.3c01953
ACS Appl. Mater. Interfaces 2023, 15, 30070−30082